nature chemical biology

REVIEW ARTICLE

PUBLISHED ONLINE: 14 FEBRUARY 2011 | DOI: 10.1038/NCHEMBIO.525

# Chemical contrast for imaging living systems: molecular vibrations drive CARS microscopy

John Paul Pezacki[1–3]*, Jessie A Blake[1,2], Dana C Danielson[1,3], David C Kennedy[1], Rodney K Lyn[1,2] & Ragunath Singaravelu[1,3]

**Cellular biomolecules contain unique molecular vibrations that can be visualized by coherent anti-Stokes Raman scattering (CARS) microscopy without the need for labels. Here we review the application of CARS microscopy for label-free imaging of cells and tissues using the natural vibrational contrast that arises from biomolecules like lipids as well as for imaging of exogenously added probes or drugs. High-resolution CARS microscopy combined with multimodal imaging has allowed for dynamic monitoring of cellular processes such as lipid metabolism and storage, the movement of organelles, adipogenesis and host-pathogen interactions and can also be used to track molecules within cells and tissues. The CARS imaging modality provides a unique tool for biological chemists to elucidate the state of a cellular environment without perturbing it and to perceive the functional effects of added molecules.**



All known living organisms are composed of complex and molecularly diverse sets of biopolymers, small molecules and ions, as well as, of course, water[1]. These biomolecules serve both structural and functional purposes and together give rise to different types of cells and tissues with varying physical attributes and primary functions[2,3]. A large proportion of living matter is composed of polymers that rely on a rather small set of monomers to create a large degree of molecular diversity. For example, polynucleotides that are made up of four simple building blocks (nucleotides) are simultaneously the source of genetic material, key players in the transcription and translation of their respective genomes[4–8], and capable of catalyzing chemical transformations[6,9,10]. Other highly abundant biomolecules include proteins, lipids[11–14] and carbohydrates[15,16], which play bifunctional roles as energy stores and recyclable structural components. Given that polymeric and self-assembled materials are key to both the structure and function of living organisms, the ability to observe them in their native environment is highly valuable. Most methods currently available for tracking molecules in living systems involve the addition of labels containing unnatural functionalities (for example, fluorophores) that provide contrast in imaging experiments. There are many strategies for the incorporation of these groups into biomolecules[1,17–19]; however, all require perturbation of the cellular environment. For this reason, it is very important to develop new label-free imaging methods based on the natural biochemical make-up of the living system under study.

Label-free methods for cellular imaging rely on inherent electronic or vibrational resonances, which provide natural chemical contrast of cellular biomolecules. Excitation of these resonances leads to phenomena such as autofluorescence, infrared absorption and Raman scattering[20]. Other label-free imaging modalities commonly used in clinical settings, including magnetic resonance imaging (MRI) and ultrasound, achieve tissue penetration but suffer from poor resolution. As such, these techniques only provide whole tissue rather than molecular information and are not useful for cell culture–based experiments. Vibrational absorption spectroscopies (for example, infrared spectroscopy) yield detailed information about the chemical bonds within a given sample. However, the low energy of the transitions involved requires excitation by longer wavelength radiation relative to fluorescence experiments. As a result, vibrational absorption microscopies generally have inherently low spatial resolution. Vibrational scattering spectroscopies including Raman scattering techniques offer slightly better resolution with similar information about the unique chemical bonds within a given sample but suffer from low sensitivity; thus, imaging requires high laser power and long acquisition times, which are incompatible with live-cell imaging[21]. Poor sensitivity in Raman scattering detection can be overcome using enhancement techniques such as surface-enhanced Raman scattering[22–25], which gives near–single molecule sensitivity for biological imaging but involves labeling, typically with functionalized metal nanoparticles[26–29]. On the other hand, CARS, which is a nonlinear optical version of Raman scattering (**Box 1**, **Fig. 1**), offers the same natural chemical contrast as linear Raman but with much better sensitivity[21,30–32]. As a result of the pioneering work in this field by X.S. Xie and coworkers, it is now possible to obtain Raman images of live cells nondestructively[32]. CARS microscopy, being a multiphoton method, also has very high spatial resolution typical of other multiphoton microscopies. Although there are distinct Raman scattering signals for peptides and nucleic acids that are clearly visible when using Raman imaging techniques on cells (**Box 1**), the strongest signal arises from lipidic C-H bond stretches. Thus the vast majority of applications of CARS microscopy to date have involved lipid imaging. Although this may seem limiting at first, the roles of lipids are so numerous and diverse in biology that the ability to image them has provided insight into a vast diversity of processes. Lipids make up all cellular membranes, control phenomena that are critical for cell signaling and function and mediate processes such as entry and secretion within a cell[11–13,33–36]. Lipids are also an important source of raw materials and energy. The dysregulation of lipid biogenesis, storage and metabolism can give rise to a number of disease states including obesity, diabetes, cardiovascular disease, neurodegeneration and cancer[37]. The details of these processes are not fully understood, their study having been stagnated by the

[1]Steacie Institute for Molecular Sciences, National Research Council of Canada, Ottawa, Canada. [2]Department of Chemistry, University of Ottawa, Ottawa, Canada. [3]Department of Biochemistry, Microbiology and Immunology, University of Ottawa, Ottawa, Canada. *E-mail: john.pezacki@nrc.ca

inherent difficulty in studying lipids. Past methods such as Nile red staining or lipid extraction have allowed visualization and component analysis separately, but researchers have never easily been able to track lipids dynamically in living systems. Thus, CARS microscopy fills a very important and long-vacant niche in studying lipid biology.

As CARS microscopy can image lipids and other molecules in cells with excellent chemical contrast, this technique has been used in a wide variety of applications. CARS microscopy has proven to be an invaluable tool for examining metabolic changes in cells including changes in lipid storage, organelle transport and aspects of lipid droplet biology[38–50]. It is well known that metabolism is affected during the development of various types of cancer, and CARS microscopy has recently emerged as a way to image these nonstatic changes[51]. CARS microscopy has also proven to be an important tool for imaging neurons and brain slices as well as investigating diseased states associated with demyelination[52–58]. This tool has also been used to investigate stem cell differentiation[59], host-pathogen interactions[39,43,48,60–65] and the effects of drugs on target cells and tissues[38,40,43,53,66–69]. Over the last decade we have seen CARS microscopy begin to have an impact on the field of chemical biology. As the details of the technique have been reviewed elsewhere[21,30,70], this review highlights the applications of CARS microscopy to studies in chemical biology and suggests potential opportunities for the future.

## Possibilities for and limitations of CARS microscopy

As CARS microscopy is a relatively new and promising method for imaging with chemical contrast, it is tempting to propose that it may be a solution to many long-standing challenges in imaging and microscopy. However, it is important to realize the limitations of this tool. In this section, we outline the scope of CARS

### Box 1 | The CARS phenomenon

Raman scattering spectroscopy detects the vibrations inherent in molecules without the need for dyes or fluorescent labeling. The signals generated result from inelastic scattering of photons with an energy shift that is characteristic of specific molecular vibrations (**Fig. 1a**, upper panel, and **Fig. 1b**, left panel). Despite the obvious appeal for biological imaging, single-photon Raman imaging has been limited by low signals because the majority of photons are scattered elastically (no energy shift). The advent of coherent Raman spectroscopy brings many advantages, prominent among them a thousand-fold improvement in signal intensity. The phenomenon of coherent anti-Stokes Raman scattering occurs when a target molecule is irradiated using two short-pulse laser beams, the pump beam and the Stokes beam. Importantly, the frequencies of these two beams must be tuned such that the frequency difference corresponds to a vibration of the target. When this condition is met, coherently vibrating molecules in the probe volume (that is, the focal point of the pump and Stokes beams) will scatter the probe beam, resulting in a coherent signal with a higher frequency than that of the probe beam and a much higher intensity than the signal from spontaneous Raman scattering (**Fig. 1a**, lower panel, and **Fig. 1b**, right panel).

The greatest advantage of CARS, its basis in inherent molecular vibrations, also represents one of its greatest limitations. To achieve natural contrast with CARS, it is necessary to have a high concentration of the same molecular moiety. For this reason, lipids, with their long aliphatic chains full of $-CH_2$ groups, are perfectly suited to CARS imaging. This is quite apparent when examining the individual Raman spectra of cellular components (**Fig. 1c**). The largest signal present in the Raman spectrum of the whole cell is from the C-H stretch of each component but is predominantly from the lipid (fat) component. Conveniently, lipids are also one of the biomolecules that can benefit from label-free imaging by CARS microscopy. Their size is on par with or smaller than the size of most common fluorescent labels, so lipid labeling is likely to perturb both lipid function and transport. Also apparent from the spectra in **Figure 1c** is the potential to use smaller Raman labels with Raman signals in the "silent region," for example –CD or –CN.

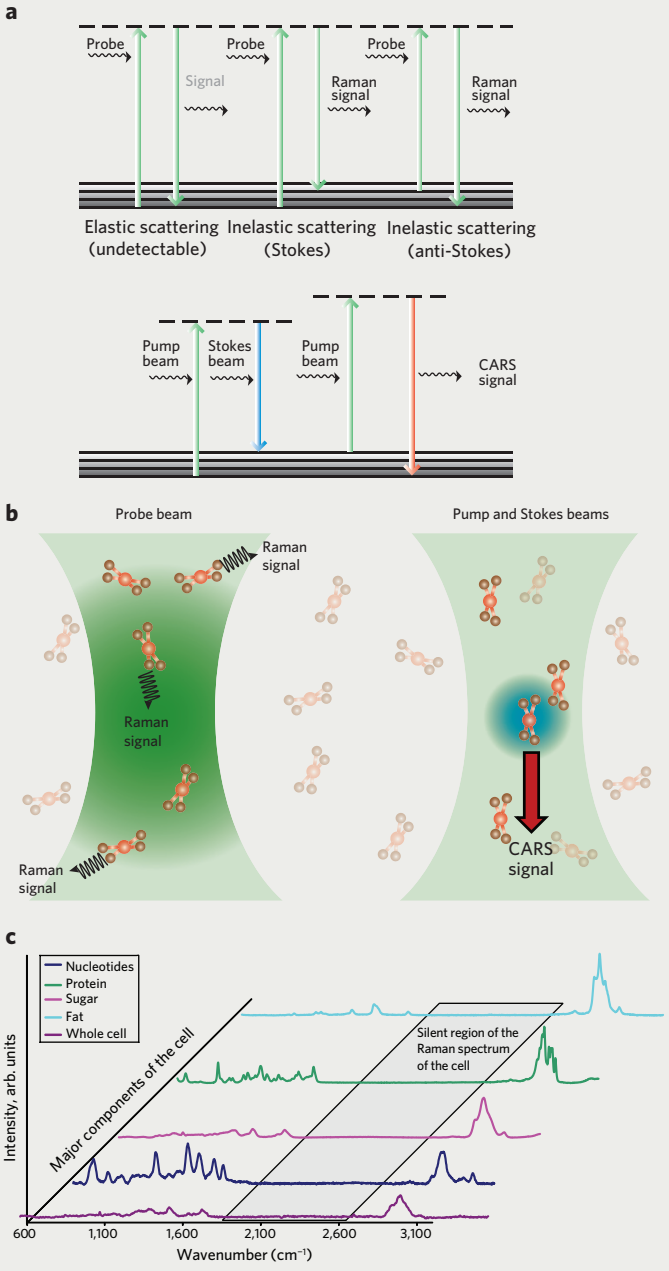


**Figure 1 | How CARS microscopy works.** (**a**) Schematic diagram of the transitions involved for Raman spectroscopy (top) and CARS spectroscopy (bottom). Both the pump beam and the Stokes beam are required to obtain a CARS signal. (**b**) Schematic illustration showing linear Raman scattering of the probe beam (left) and nonlinear coherent anti-Stokes Raman scattering (right). (**c**) Raman spectra corresponding to various cellular components.

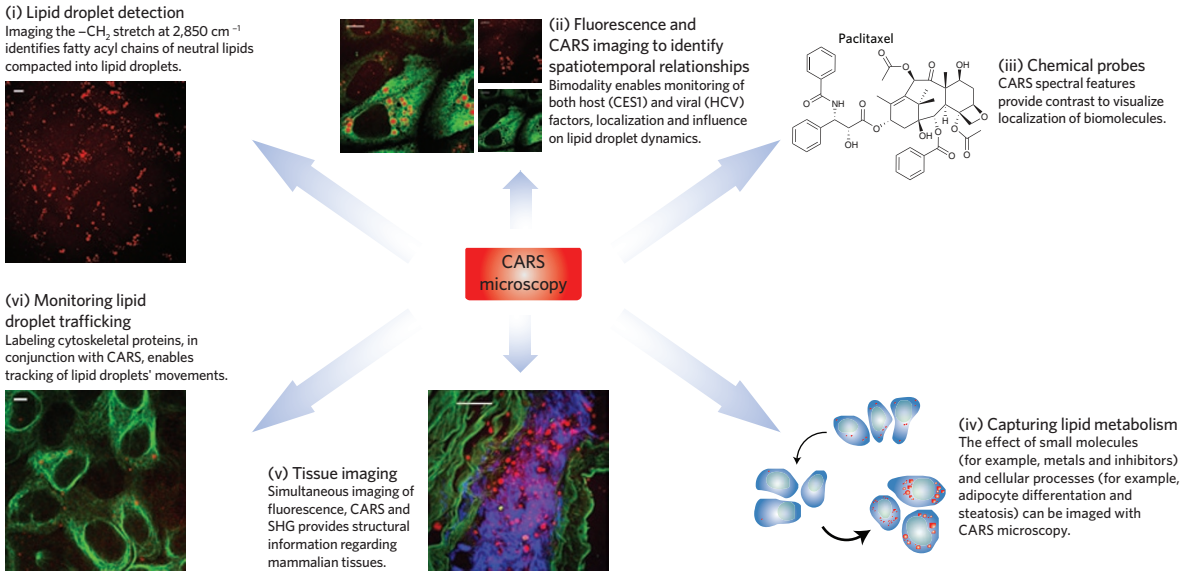


**Figure 2** | **Applications of CARS microscopy.** Applications of CARS microscopy are shown for the label-free imaging of molecules in various systems. Clockwise from top left: (i) Lipid droplet detection: CARS image shows naïve Huh7 cells' lipid content. (ii) Monitoring host and viral factor localization and their influence on the lipid phenotype using immunofluorescence with CARS: CARS/TPF overlay image shows overexpressed liver protein CES1 that is involved in processing neutral lipids in lipid droplets and implicated in HCV replication and infection[92]. (iii) Tracking chemical probes: CARS active functionalities provide direct detection of molecules, such as paclitaxel, label-free. (iv) Detection of lipid phenotype changes due to small molecules, or due to cellular processes, as shown by the schematic of mouse fibroblast differentiation into adipocytes[45]. (v) Tissue imaging: image shows rabbit aorta (green, smooth muscle elastin; red, lipid droplets; blue, collagen); image reprinted with permission from ref. 75. (vi) Tracking dynamics of lipid droplets: image shows Alexa-488 labeling of tubulin with adjacent lipid droplets in cargo transport; in conjunction with CARS enables measurement of changes in lipid droplet dynamics. The scale bars for the cell images are 10 μm and 50 μm for the tissue image in (v).



microscopy so that an appreciation of its true capabilities and potential applications can be highlighted. With the high spatial resolution typical of multiphoton microscopies and fast image acquisition rates, CARS microscopy has proven to be an excellent imaging modality for monitoring C-H vibrational stretches in lipids and O-H stretches in water. However, because this is a nonlinear technique that depends on three photons to coherently stimulate a resonance frequency, the CARS signal depends on the square of the concentration of vibrational oscillators in the focal volume of the material being imaged. For this reason, the enhanced sensitivity associated with CARS drops off quickly with decreasing oscillator concentration, and the imaging of less abundant biomolecules is difficult. Although it is difficult to define a detection limit because of the different methods for performing CARS microscopy, typically $10^5$ to $10^6$ oscillators per focal volume produce sufficient contrast, making this a much less sensitive technique than fluorescence imaging.

CARS images often show some spectral distortion and limited sensitivity arising from unwanted background signals (referred to as nonresonant background)[21,30,70]. Because of these issues, quantifying CARS signals can present a challenge. There are, however, tools available to achieve relative quantification. Changes in signal intensity relative to control samples, even if semiquantitative in nature, can give important information about biological phenomena over time in living systems. In some of the examples we will discuss, image analysis algorithms have been applied to correct for the nonlinear effects of CARS microscopy[38,62,71]. Another approach that has been used for the analysis of CARS images is called voxel analysis[39,40,43,72]. This tool calculates signal intensity within a field of view as a function of pixel volume, and only those pixels that meet a minimum threshold signal are counted[39,40,43,72]. Using methods such as these for the systematic analysis of CARS images allows for the quantification of changes that are independent of unwanted background signals. For most applications of CARS microscopy, the intensity of the CARS signal is not the only important observable criterion in studying biological processes. Changes in features such as size, spatial distribution and morphology do not necessarily involve significant changes in the concentration of vibrational oscillators in the focal volume. These features are often as important, if not more important, than the intensity of the signal in terms of understanding a chemical or biochemical event. Many of the examples highlighted within this review fall into this category.

Recently another coherent Raman microscopy called stimulated Raman scattering (SRS) has emerged[73,74]. Although many of the issues that are of concern with CARS microscopy, such as the nonlinear dependence of the signal with respect to analyte concentration and high background signals, are overcome with SRS, it remains a very difficult approach to employ, with significant technical barriers, and no commercial SRS microscope currently exists. On the other hand, because a commercial CARS microscope based on a set-up described by Pegoraro *et al.* is currently available[75], CARS microscopy is broadly accessible to researchers in a number of fields including chemical biology; this opens up new avenues for label-free imaging with chemical contrast.

## Visualizing the effects of molecules

The potential of CARS microscopy to improve our understanding of lipid metabolism and fat storage has been demonstrated in multiple ways with lipid droplets[38], cells[42,47], tissue samples[71,75–77] and even live organisms[39,78] (**Fig. 2**). As described in **Box 1**, the imaging of lipids can be accomplished by simply tuning the resonance frequency to the spectral region in which C-H bond vibrations are observed, thus allowing visualization of lipids and lipid-rich structures as well as direct measurement of the effects small molecules and metabolites have on lipids. For instance, a recent study compared the growth of lipid droplets in the liver by CARS microscopy in mice fed a diet lacking methionine and choline compared with those fed a regular diet[76]. Methionine and choline deprivation is

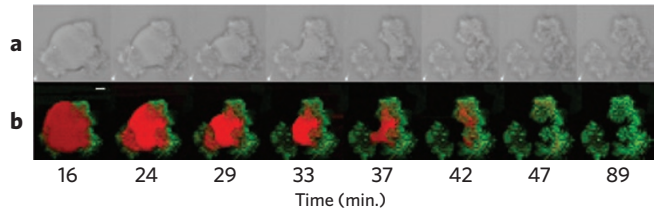


**Figure 3 | Digestion of a glycerol trioleate droplet by porcine pancreatic lipase.** (**a**) Bright-field microscopy images. (**b**) False-color images obtained by CARS microspectroscopy showing glyceryl trioleate (red) and its lipolytic products (green). Scale bar = 5 μm. Reproduced with permission from ref. 38. Copyright 2010 American Chemical Society.

known to impair very low–density lipoprotein (VLDL) production, which leads to impaired triglyceride secretion and an accumulation of hepatic fat[76]. CARS microscopy made it possible to directly measure the growth of lipid droplets caused by lowered levels of methionine and choline for intact tissue sections.

The effects of drugs that target pathways involved in lipid metabolism have also been investigated using CARS microscopy, including a study of lysophosphatidylcholine and other pharmacological agents on demyelination and neurodegeneration[55,79]. Similarly, specific gene knockdown through RNA interference (RNAi) can be used in conjunction with CARS microscopy to elucidate the role of specific gene products involved in lipolysis. RNAi and CARS microscopy revealed that CGI-58, a protein that facilitates lipolysis of lipid droplets, is not involved in hormone-stimulated lipid droplet remodeling[80]. By dynamically tracking the cellular response to gene knockdown and lipolytic stimulation with CARS microscopy, the authors obtained previously unattainable time-course data with high resolution that revealed new insights into *de novo* lipid-droplet formation and clarified the role of CGI-58 (ref. 80). Another study used CARS microscopy to follow adipogenesis and gene regulation induced by the small molecules isobutylmethylxanthine and dexamethasone during differentiation[81]. All of these studies demonstrate the potential of CARS microscopy to elucidate the function and cellular consequences of small molecules in live tissue.

In our lab, CARS microscopy has been used to probe the link between copper and lipid metabolism[40]. This link has been previously observed for Wilson's disease using gene knockout studies with mice; however, our study is the first direct observation of the effect copper has on lipid density[82]. CARS images revealed that cells exposed to uncomplexed copper ($CuCl_2$) exhibited only a slight increase in lipid density, whereas exposure to either copper complexed with EDTA (Cu(EDTA)) or histidine ($Cu(his)_2$), a bioavailable form of copper, resulted in a marked increase in lipid density. This demonstrated the significant effect that overexposure to complexed copper has on lipid metabolism as well as the relevance of the ligand to cellular uptake of the different copper complexes[40].

In another study, we used CARS microscopy to probe the cellular consequences of exposure to copper catalysts commonly used in [3+2] cycloadditions between alkynes and azides ('click' reactions)[1,83] for bioconjugation. Toxicity, the effects on lipid metabolism, the level of copper uptake and the ability to catalyze reactions on live cells were characterized for $CuSO_4$, Cu-SBP (sulfonated bathophenanthroline), Cu-TBTA (tris((1-benzyl-1H-1,2,3-triazol-4-yl)methyl)amine) and $Cu(his)_2$ (unpublished data). By exploring the biological effects and potential utility of copper catalysis in living systems, these results open the possibility of developing tailored catalysts specifically for applications in living systems.

In some cases, it is desirable to follow specific exogenous molecules rather than endogenous lipid features. Introduction of a label into these molecules makes it possible to track them with CARS imaging. Ideally the label should possess a vibration in the Raman silent region of the cell (**Box 1**) without altering any other properties. Perhaps the best example of such a label is the replacement of hydrogen by deuterium. This strategy was employed to help elucidate the health benefits imparted by fish oil that arise from polyunsaturated fatty acids such as oleic acid and eicosapentaenoic acid (EPA)[84]. The $-CD_2$ vibration in deuterated oleic acid is 2,105 $cm^{-1}$, significantly shifted from the $-CH_2$ in non-deuterated oleic acid, which appears at 2,850 $cm^{-1}$ (ref. 84). In the presence of EPA, deuterated oleic acid and EPA were found to colocalize within lysosomes in the form of triglycerides. In the absence of EPA, oleic acid did not accumulate in lysosomes, thus shedding light on how such polyunsaturated acids participate in lipid metabolism and what processes lead to the observed health benefits. Deuterated small molecules have also been used to show the signal-to-noise benefits of frequency modulation CARS[85] for studying membrane partitioning in a nonperturbative manner[86] and for monitoring aquaporin function in the diffusion of water[87]. In general, isotopic labeling provides a highly convenient way of tracking exogenous molecules.

One of the significant advantages CARS microscopy offers is the wealth of information it can provide for one system under study. For example, as will be discussed in a subsequent section, whole-tissue imaging can be complemented by simultaneous subcellular imaging. In addition, multiplex CARS spectroscopic imaging provides detailed information on the chemical composition of the sample, measuring the Raman spectrum for each submicron pixel of the CARS image. By using multiplex CARS tuning to two different vibrational signatures (C=C and C-H stretches), one study successfully quantified the degree of fatty acid unsaturation and the amount of acyl chain order in HeLa cells and adipocytes[71]. Recently the enzymatic functions of proteins involved in lipolysis have also been monitored by multiplex CARS[38]. Triglycerides within lipid droplets were shown to be distinguishable from their lipolysis products on the basis of the characteristic Raman signals for each molecule[38]. Multiplex CARS was used to carry out component analysis of the digestion of glyceryl trioleate by porcine pancreatic lipase into its lipolytic products *in vitro*. Changes in the CARS spectrum between 2,800–3,100 $cm^{-1}$ gave quantitative information about the rate of digestion within a lipid droplet[38]. Hyperspectral analysis of the Raman spectrum of each pixel allowed quantification of the different chemical components, whereby the spectra are deconvoluted (treated as a linear combination of the component spectra) and the relative concentration of each component is visualized as a false color image (see **Fig. 3 (ref. 38)**). This technique was also used to distinguish between the bioactive molecules ergosterol, progesterone and vitamin D contained within lipid droplets to aid in understanding the physiological transport and absorption of these molecules as well as their effects on lipolysis[38]. It should be noted that Raman spectra obtained via CARS imaging are more complex than those from linear Raman spectroscopy and therefore require higher level analysis. However, the data treatment used in the above examples should be able to distinguish any set of molecules with distinct Raman signals. As such, multiplex CARS is becoming an increasingly attractive tool in chemical biology, providing all the benefits of CARS microscopy with detailed Raman spectroscopic data.

Although the majority of applications in chemical biology using CARS microscopy involve lipid imaging, the technique is certainly not limited to lipids. Any molecular oscillator can be monitored by CARS, provided it is found in sufficiently high local concentrations to give chemical contrast. For example, CARS microscopy has been applied to monitoring drug release from polymer and bead samples used as drug delivery agents. In this case, both the delivery agent and drug must have unique vibrational modes that can be used to individually identify and monitor them. Paclitaxel release has been studied in this manner[66].

Raman vibrations that arise from the aromatic groups within the drug and that are absent in the surrounding poly(ethylene glycol)/poly(lactic-co-glycolic acid) (PEG/PLGA) polymer coatings were used to follow the drug changes in the release over time from a coated polymer by CARS microscopy. This allowed researchers to study how changes in the polymer composition affected the rate of drug release into solution. Recently, this approach was applied to monitoring the release of theophylline (dimethylxanthine), a drug commonly used to treat respiratory conditions, from solid lipid-based tablets upon dissolution in an aqueous medium[69].

As CARS microscopy is well suited to live-cell imaging, we have only begun to realize its potential to visualize dynamic processes during drug delivery and to aid in characterization in physiologically relevant settings. There remain a wealth of possibilities for its use in many other imaging applications in which chemical information and contrast are useful. The above examples highlight the application of CARS microscopy to monitoring dynamic biochemical processes in response to chemical perturbation.

## Multimodal CARS microscopy and host-pathogen interactions

A powerful asset of CARS microscopy is its ability to be used in conjunction with other two-photon imaging modalities. In particular, when a femtosecond laser is employed, the excitation source is amenable to inducing both the CARS and the two-photon fluorescence signals. Thus, both systems can be combined into one microscope, thereby allowing the collection of real-time information from the same sample window using both modalities, as well as streamlining data collection. There is particular benefit from this approach in monitoring host-pathogen interactions. By summarizing the most recent discoveries in the field, we aim to highlight the possibilities offered by multimodal CARS to chemical biology.

The interactions of pathogenic organisms such as viruses and bacteria necessarily involve interactions at cellular membranes for, at the minimum, the entry of the pathogen into its host cell to begin infection[88]. Many pathogens also alter their environment in a way that changes the internal make-up, metabolic processes and energy requirements of an infected cell[88]. Indeed, nearly all viruses of concern to human health have some specific interactions with lipids, including human immunodeficiency virus (HIV), hepatitis C virus (HCV) and the influenza virus[88]. Viruses that modify the host cell to further their propagation are also common[88]. For instance, infection with most positive-sense RNA viruses, including dengue virus, severe acute respiratory syndrome (SARS) virus and HCV, results in modification of the membranous ER[89]. As HCV also modulates many other facets of lipid metabolism to facilitate its viral life cycle[61], including viral particle assembly around lipid droplets[90] and viral particle secretion using components of the VLDL pathway[91], there is great potential for applying CARS microscopy to study host-virus interactions in HCV and other viral infections.

CARS microscopy in combination with two-photon fluorescence (TPF) microscopy has been applied to the visualization of spatiotemporal relationships between HCV RNA and alterations in host-cell lipid metabolism[62]. In this study, replication-competent HCV RNA was chemically labeled at the 5′ end with a fluorophore and subsequently monitored in living cells using TPF microscopy while changes to the host cell lipid content were simultaneously monitored using CARS microscopy; changes in lipid metabolism as a function of HCV RNA were then quantified[62]. Increasing lipid density was observed in hepatoma cells expressing the HCV RNA[62]. This initial study demonstrated the multimodal approach's value for simultaneous dynamic tracking of the subcellular localization of viral RNA while establishing the perturbed lipid phenotype. It became apparent that CARS microscopy would have similar utility in studying the effects of host and viral genes as well as the effects of small-molecule inhibitors on the viral life cycle in real time.

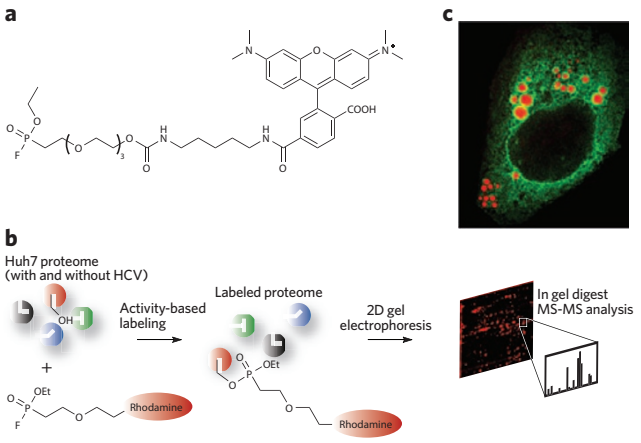


**Figure 4 | Identifying carboxylesterase 1 as a host factor involved in the hepatitis C virus life cycle.** (**a**,**b**) CES1 was discovered to be an important enzyme for HCV infection through the use of the fluorophosphonate activity-based protein profiling probe (**a**), following the general scheme in **b**[92]. CES1 is a trimeric serine hydrolase enzyme that modifies lipid droplet content. (**c**) The enlargement of lipid droplets (red) is shown in Huh7.5 human hepatoma cell lines by the human protein CES1 (green). CES1 enzyme activity was shown to give rise to very large lipid droplets that both enhance HCV replication and favor HCV viral particle assembly.

CARS microscopy in conjuction with TPF microscopy was subsequently used to examine the effects of lipid metabolism–associated host gene expression on HCV propagation. Peroxisome proliferator-activated receptor alpha (PPARα) antagonism was shown to create an antiviral state, judging from the observation that both siRNA and chemical knockdown created a hyperlipidemic condition that correlated with an antiviral state[64]. Similarly, CARS microscopy was instrumental in understanding the role of host factor carboxylesterase 1 (CES1) as a proviral gene that is upregulated upon HCV infection (**Fig. 4**)[92]. The tool allowed for correlation between CES1 levels in hepatoma cells and the size and density of lipid droplets, which are necessary for the functional VLDL pathway and are a likely vehicle for HCV particle assembly and secretion. The multimodal strategy allowed for a better understanding of CES1's role, as the host factor was found to concentrate around lipid droplets near the endoplasmic reticulum, suggesting the protein loading of neutral lipids to ER-associated lipid droplets is crucial for HCV replication and maturation of HCV virion. Several studies have shown the liver-specific microRNA miR-122 is a key regulator of cholesterol biosynthesis as well as of HCV replication[93–96]. Thus, we are currently using CARS microscopy to investigate the role of miR-122 and other miRNAs in modulating hepatic lipid content and lipid droplet morphology.

CARS and TPF microscopies were also used to examine the HCV antiviral mechanism of small-molecule modulators, including modulators of the mevalonate pathway[97] and PPAR signaling pathways[43]. HCV viral replication and particle assembly is thought to be localized to the interface between ERs and lipid droplets. Using live cell imaging techniques, it was shown that HCV replication complexes are dispersed by modulating the mevalonate pathway using lovastatin and the PPAR signaling pathway using a PPARα antagonist, most likely by preventing the lipidation of a host protein, FBL2, that has a known association with the HCV replication complex[43]. This multimodal strategy lent itself to a kinetics-based comparison of the drugs' effects, as the study revealed the PPARα antagonist mediated its dispersion of HCV RNA at a much faster rate than lovastatin did[43].

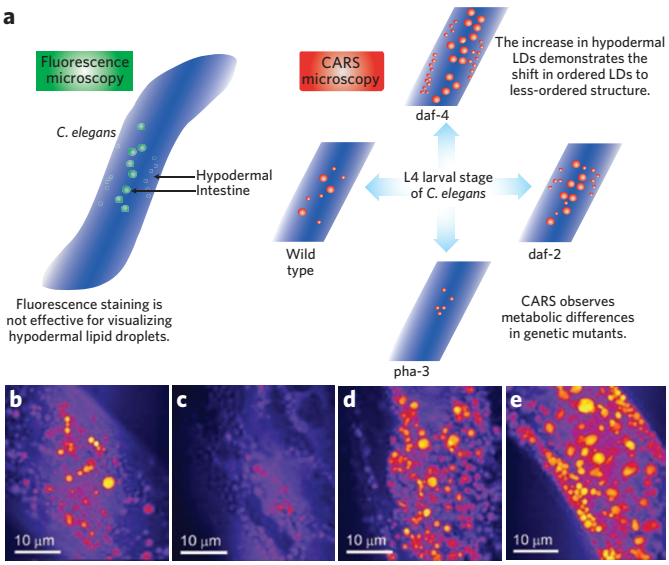


**Figure 5 | Monitoring lipid storage in *Caenorhabditis elegans*.** (**a**) The schematic shows the advantages of CARS microscopy over fluorescence methods in imaging lipid droplets and lipid metabolism in *C. elegans*. Differences in lipid droplet distributions that can be observed by CARS microscopy and that are not possible to visualize by fluorescence in genetic mutants of *C. elegans* are represented schematically[39,65]. (**b**–**e**) CARS microscopy images show differences in lipid droplet density for the wild-type *C. elegans* (**b**), the pha-3 mutant (**c**), the daf-2 (**d**) and the daf-4 (**e**) mutants. The scale bars are 10 µm. The images were reproduced with permission from ref. 39.

More recently, this bimodal strategy was adapted to include differential interference contrast microscopy, which enabled examination of the dynamics of the HCV core protein's interaction with lipid droplets[72]. It was shown that the HCV core protein can rapidly induce lipid droplet biogenesis in living cells and that the HCV core protein also has a dramatic influence on the speed and directionality of lipid droplet movement, presumably as part of a mechanism by which HCV viral particle assembly is initiated[72].

Although the application of CARS microscopy to host-pathogen interactions is in its infancy, researchers are beginning to apply this technique to viruses other than HCV. For example, a recent study used CARS microscopy to examine the infection of fibroblast cells by cytomegalovirus (HCMV), also known as human herpesvirus 5 (HHV-5)[48]. HCMV is a double-stranded DNA virus that is potentially life threatening in immunocompromised patients. CARS microscopy was used to examine mouse HCMV infection of NIH/3T3 fibroblast cells, tracking morphological changes in cells such as expanded nuclei and altered lipid droplet distributions[48]. Infection with HCMV-GFP fusion constructs and imaging with TPF microscopy allowed for the simultaneous tracking of viral proteins during infection so that morphological changes could be correlated with the degree of HCMV infection[48]. These results clearly show the potential of CARS microscopy to elucidate new mechanistic details, correlate metabolic changes in a cell with the levels of infection and measure dynamics in the detailed examination of host-pathogen interactions. It is expected that many more applications in this field will be discovered in the near future.

## Toward clinical imaging

CARS presents unique opportunities for tissue imaging that allow for more detailed studies of biological systems and the effects of small-molecule treatment and may also have clinical applications in the future. As a nondestructive, label-free modality that achieves subcellular resolution with chemical specificity, CARS is quite suitable for tissue imaging. Furthermore, deep penetration of thick and turbid specimens is possible because of near infrared excitation, and the nonlinear dependence of the signal on excitation intensity gives inherent three-dimensional optical sectioning. Already the usefulness of CARS microscopy has been demonstrated in tissue imaging, predominantly using the high contrast of the C-H stretch for lipid imaging.

Live animal imaging using CARS microscopy was first applied to the imaging of skin tissue in mice using video rate imaging methods[78]. This was accomplished with backscattering of the CARS signal in a given tissue that yields an 'epi-CARS' signal. CARS imaging and spectroscopy of lipid-rich tissue structures in the skin of living mice allowed for the direct observation of sebaceous glands, corneocytes and adipocytes with high contrast and subcellular resolution[78]. Notably, this technique allowed for the observation of dynamic processes. Diffusion of oils into the skin of mice could be observed without the addition of a label because of the contrast achievable using the C-H vibrational band[78]. The changes in the distribution of the oil were monitored, and it was found that penetration only occurred through the stratum corneum, not into dermis, suggesting that the oil could not diffuse farther than the epidermal layer of the mouse skin. This represents the first direct, label-free imaging of an exogenously added small molecule in the tissues of a live animal by CARS microscopy.

Live animal imaging has been conducted with the organism *Caenorhabditis elegans*[39]. *C. elegans* serves as an excellent model organism because of its small size and the ease of whole-body imaging and also because its genetics have been extensively studied. As a result, there are a number of functionally relevant knockout strains available that perturb lipid metabolism through mechanisms similar to those that occur in higher order eukaryotes. *C. elegans* was used to examine the details of metabolic diseases that involve changes in lipid stores on the single-cell level *in vivo*[39]. Interestingly, CARS microscopy was able to visualize hypodermal lipid droplets that were not visible or quantifiable by other methods (**Fig. 5**)[39]. Specifically, the technique was used to quantify changes in lipid stores in genetic mutants in which metabolic pathways affecting lipid storage had been previously established. A feeding-defective mutant called pha-3 showed a decrease in lipid content of approximately one-third compared to that of control organisms, as measured by lipid volume fraction[39]. In contrast, other mutants such as daf-2 and daf-4 with impaired insulin growth factor and transforming growth factor signaling pathways, respectively, showed significantly increased lipid volumes, a change in lipid phase and an increased number of lipid droplets in hypodermal cells[39]. This example highlights one of the advantages label-free imaging has over fluorescent labeling and staining. The researchers were unable to observe hypodermal lipid droplets via Nile red fluorescence. The authors attributed this to one of two factors: either the Nile red reaches these lipid droplets less efficiently (metabolic effect) or the fluorescence is less efficient in the environment of the hypodermal lipid droplets (photophysical effect). Further mutants have subsequently been studied[65], and the results emphasize CARS microscopy's utility in measuring lipid phenotype and also in predicting genotypes in mutant organisms that are models for genetic diseases.

CARS microscopy is also well suited to imaging nerve tissue; the myelin sheath that coats nerve axons is lipid rich and thus gives excellent contrast[57] (**Fig. 6a,b**). Real-time imaging of intact myelin by CARS has helped elucidate the cellular mechanisms of demyelination disorders, which would not be possible with methods that require fixed tissue, such as electron microscopy and immunofluorescence[55]. Additionally, CARS has potential for *in situ* brain imaging. Thus far, high-resolution images of brain structures from an unfixed mouse brain slice have allowed identification of a large brain tumor with the same spatial accuracy of tumor margins as in histological staining[54].

Other clinically relevant applications of CARS microscopy include the quantification of lipid-content for intact tissues. As mentioned previously, CARS microscopy has been successfully applied to visualizing mouse liver tissue[76]. Assessing tissue lipid content with CARS microscopy is also relevant in cancer pathology[51]. CARS is currently being used to understand the link between obesity and breast cancer. Using this technique, it has been shown that the mammary glands of obese rats contain elevated levels of adipocytes with increased sizes of lipid droplets[98]. By combining CARS, second harmonic generation and TPF, the authors were able to image several components of the mammary stroma, thus lending insight into the dynamics of the tumor microenvironment. Furthermore, CARS has been used to probe the association of lipid-rich tumors with increased tumor metastasis, tracking intracellular lipid accumulation in primary, circulating and metastasized cancer cells[51].

Lipid metabolism also plays a key role in atherosclerosis[41,77,99]. As such, CARS microscopy may prove to be very valuable in the study of the disease, improvement in diagnosis and discovery of new treatments. To aid in understanding the pathogenesis of plaque vulnerability, multiplex CARS spectroscopy has been used to identify and characterize the chemical profiles of four types of atherosclerotic lipids (**Fig. 6c–f**)[41]. Prior to this application of CARS, such information was only available through indirect analyses after sample removal and processing or via dissection imaging. The effect of statin drugs on the chemical profiles of the plaques was also measured with specific reference to plaque stability. Although the morphologies of lipid-rich features remained unchanged, the chemical composition of each feature was quite different for cells treated with statins[41]. After eight weeks of treatment with simvastatin, lipid crystals were less solidified, as evidenced by a decrease in the signal intensities assigned to the asymmetrical $-CH_2$ and $-CH_3$ vibrations[41].

CARS is currently capable of tissue penetration from 30–120 μm, but constant improvements in optics are achieving greater penetration with lower levels of nonresonant background. Also, CARS endoscopy has been on the horizon since the recent development of a fiber-delivered probe able to collect the back-scattered, forward-generated CARS signal in biological tissues[100]. A CARS endoscope will provide access to deeper tissues *in vivo,* inviting a wealth of applications in clinical diagnostics such as *in situ* imaging of tumor margins and atherosclerotic plaques, among others. It is clear that CARS has a future in clinical imaging. CARS is able to fill the role of histological staining and biochemical analysis in several applications, achieving the same result while avoiding tissue fixation and use of reagents. Furthermore, CARS complements MRI applications, as it is a label-free and nondestructive modality. Although CARS cannot match the tissue penetration that MRI provides, it achieves far greater resolution. The ability of CARS to be used simultaneously with other imaging modalities makes it particularly attractive.

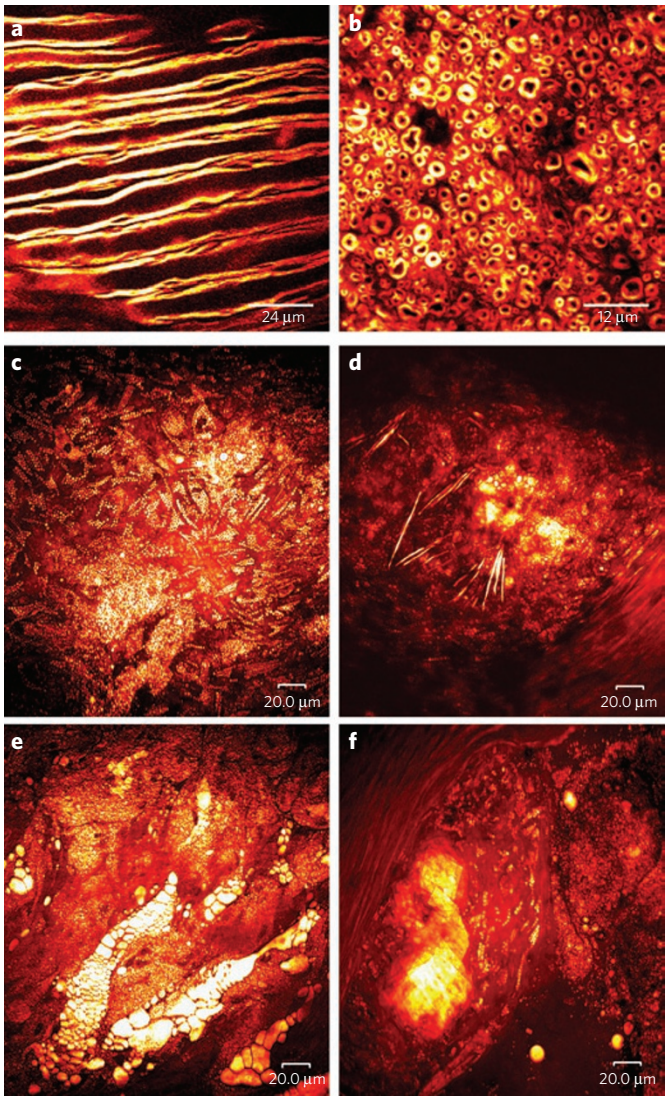


**Figure 6 | Tissue imaging using CARS microscopy.** (**a**,**b**) White matter from a rat brain. (**a**) CARS microscopy images of fixed myelin sheaths from the coronal plane of the lumbar spinal enlargement and (**b**) from a mechanically cut transverse section, both acquired with the excitation beams circularly polarized to remove polarization artifacts. Images courtesy of E. Bélanger, S. Laffray and D. Côté. (**c**–**f**) Label-free, lipid-selective CARS imaging of atherosclerotic lipids are shown for atherosclerotic lesions with four types of atherosclerotic lipids shown: (**c**) intracellular lipid droplets in foam cells, (**d**) needle-shaped lipid crystals, (**e**) extracellular lipid deposits and (**f**) plate-shape lipid crystals. The bright yellow color indicates CH bond–rich lipids. Images courtesy of S-H. Kim, J.Y. Lee, E.S. Lee, D.W. Moon.

## Outlook

The most powerful aspect of CARS microscopy is that it can report with high resolution on the chemical and biological nature of any sample using inherent Raman vibrational resonances, provided the resonances are sufficiently distinct and in high enough local concentration. Many of the applications of CARS microscopy to date have focused on imaging lipids and monitoring their phenotypic changes in response to a chemical or biological perturbation. The themes highlighted in this review speak to the relevance of results obtained with CARS microscopy to problems in health and disease and highlight the opportunities for further investigation both in terms of imaging and discovery. CARS microscopy increases the repertoire of today's chemical biologist and, notably, provides the previously unavailable ability to dynamically monitor biological systems with chemical specificity. Additionally, there remains great potential for this technique to image exogenous molecules, to perform high-throughput screening and to visualize chemical reactions that are of relevance to biology. Constant improvements in methods related to CARS microscopy (such as SRS microscopy) and in optics are increasing its capacity to image less abundant target molecules and expanding the possible applications of this technique. These advances are also driving the progress toward exciting clinical imaging applications. Given the recent commercialization of a CARS microscope, based on the design by Pegoraro *et al.*[75], and thus the increased accessibility of the technique, we envision its routine usage in a wide variety of fields in the near future.

## References


1. Prescher, J.A. & Bertozzi, C.R. Chemistry in living systems. *Nat. Chem. Biol.* **1**, 13–21 (2005).
2. Rafii, S. & Lyden, D. Therapeutic stem and progenitor cell transplantation for organ vascularization and regeneration. *Nat. Med.* **9**, 702–712 (2003).
3. Zaret, K.S. Regulatory phases of early liver development: Paradigms of organogenesis. *Nat. Rev. Genet.* **3**, 499–512 (2002).
4. Ban, N., Nissen, P., Hansen, J., Moore, P.B. & Steitz, T.A. The complete atomic structure of the large ribosomal subunit at 2.4 angstrom resolution. *Science* **289**, 905–920 (2000).
5. Fischer, N., Konevega, A.L., Wintermeyer, W., Rodnina, M.V. & Stark, H. Ribosome dynamics and tRNA movement by time-resolved electron cryomicroscopy. *Nature* **466**, 329–333 (2010).
6. Kozak, M. Initiation of translation in prokaryotes and eukaryotes. *Gene* **234**, 187–208 (1999).
7. Schmeing, T.M. & Ramakrishnan, V. What recent ribosome structures have revealed about the mechanism of translation. *Nature* **461**, 1234–1242 (2009).
8. Sund, J., Ander, M. & Aqvist, J. Principles of stop-codon reading on the ribosome. *Nature* **465**, 947–950 (2010).
9. Ditzler, M.A., Aleman, E.A., Rueda, D. & Walter, N.G. Focus on function: single molecule RNA enzymology. *Biopolymers* **87**, 302–316 (2007).
10. Schnabl, J. & Sigel, R.K.O. Controlling ribozyme activity by metal ions. *Curr. Opin. Chem. Biol.* **14**, 269–275 (2010).
11. Fyrst, H. & Saba, J.D. An update on sphingosine-1-phosphate and other sphingolipid mediators. *Nat. Chem. Biol.* **6**, 489–497 (2010).
12. Kutateladze, T.G. Translation of the phosphoinositide code by PI effectors. *Nat. Chem. Biol.* **6**, 507–513 (2010).
13. Pike, L.J. Lipid rafts: bringing order to chaos. *J. Lipid Res.* **44**, 655–667 (2003).
14. Pyne, S. & Pyne, N.J. Sphingosine 1-phosphate signalling in mammalian cells. *Biochem. J.* **349**, 385–402 (2000).
15. Deberardinis, R.J., Sayed, N., Ditsworth, D. & Thompson, C.B. Brick by brick: metabolism and tumor cell growth. *Curr. Opin. Genet. Dev.* **18**, 54–61 (2008).
16. Ohtsubo, K. & Marth, J.D. Glycosylation in cellular mechanisms of health and disease. *Cell* **126**, 855–867 (2006).
17. Mamidyala, S.K. & Finn, M.G. *In situ* click chemistry: probing the binding landscapes of biological molecules. *Chem. Soc. Rev.* **39**, 1252–1261 (2010).
18. Agard, N.J. & Bertozzi, C.R. Chemical approaches to perturb, profile, and perceive glycans. *Acc. Chem. Res.* **42**, 788–797 (2009).
19. Xie, J. & Schultz, P.G. Innovation: A chemical toolkit for proteins—an expanded genetic code. *Nat. Rev. Mol. Cell Biol.* **7**, 775–782 (2006).
20. Prasad, P.N. *Introduction to Biophotonics* (John Wiley & Sons, Hoboken, NJ, 2003).
21. Evans, C.L. & Xie, X.S. Coherent anti-stokes raman scattering microscopy: chemical imaging for biology and medicine. *Annu. Rev. Anal. Chem.* **1**, 883–909 (2008).
22. Campion, A. & Kambhampati, P. Surface-enhanced Raman scattering. *Chem. Soc. Rev.* **27**, 241–250 (1998).
23. Kneipp, J., Kneipp, H. & Kneipp, K. SERS—a single-molecule and nanoscale tool for bioanalytics. *Chem. Soc. Rev.* **37**, 1052–1060 (2008).
24. Qian, X.M. & Nie, S.M. Single-molecule and single-nanoparticle SERS: from fundamental mechanisms to biomedical applications. *Chem. Soc. Rev.* **37**, 912–920 (2008).
25. Willets, K.A. & Van Duyne, R.P. Localized surface plasmon resonance spectroscopy and sensing. *Annu. Rev. Phys. Chem.* **58**, 267–297 (2007).
26. Kennedy, D.C., Duguay, D.R., Tay, L.L., Richeson, D.S. & Pezacki, J.P. SERS detection and boron delivery to cancer cells using carborane labelled nanoparticles. *Chem. Commun.* (Camb.) 6750–6752 (2009).
27. Kennedy, D.C. *et al.* Nanoscale aggregation of cellular beta(2)-adrenergic receptors measured by plasmonic interactions of functionalized nanoparticles. ACS *Nano* **3**, 2329–2339 (2009).
28. Kennedy, D.C., Hoop, K.A., Tay, L.L. & Pezacki, J.P. Development of nanoparticle probes for multiplex SERS imaging of cell surface proteins. *Nanoscale* **2**, 1413–1416 (2010).
29. Hu, Q., Tay, L.L., Noestheden, M. & Pezacki, J.P. Mammalian cell surface imaging with nitrile-functionalized nanoprobes: biophysical characterization of aggregation and polarization anisotropy in SERS imaging. *J. Am. Chem. Soc.* **129**, 14–15 (2007).
30. Cheng, J.X. & Xie, X.S. Coherent anti-Stokes Raman scattering microscopy: instrumentation, theory, and applications. *J. Phys. Chem. B* **108**, 827–840 (2004).
31. Duncan, M.D., Reintjes, J. & Manuccia, T.J. Scanning coherent anti-Stokes Raman microscope. *Opt. Lett.* **7**, 350–352 (1982).
**This paper describes the first scanning CARS microscope.**
32. Zumbusch, A., Holtom, G.R. & Xie, X.S. Three-dimensional vibrational imaging by coherent anti-Stokes Raman scattering. *Phys. Rev. Lett.* **82**, 4142–4145 (1999).
**This seminal study is a landmark demonstration of CARS microscopy using near-infrared co-linear laser pulses.**
33. Ile, K.E., Schaaf, G. & Bankaitis, V.A. Phosphatidylinositol transfer proteins and cellular nanoreactors for lipid signaling. *Nat. Chem. Biol.* **2**, 576–583 (2006).
34. Mellman, I. Endocytosis and molecular sorting. *Annu. Rev. Cell Dev. Biol.* **12**, 575–625 (1996).
35. Nagle, J.F. & Tristram-Nagle, S. Structure of lipid bilayers. *Biochim. Biophys. Acta* **1469**, 159–195 (2000).
36. Resh, M.D. Trafficking and signaling by fatty-acylated and prenylated proteins. *Nat. Chem. Biol.* **2**, 584–590 (2006).
37. Moffatt, R.J. & Stanford, B.A. *Lipid Metabolism and Health* (CRC/Taylor & Francis, Boca Raton, FL, 2006).
38. Day, J.P.R., Rago, G., Domke, K.F., Velikov, K.P. & Bonn, M. Label-free imaging of lipophilic bioactive molecules during lipid digestion by multiplex coherent anti-Stokes Raman scattering microspectroscopy. *J. Am. Chem. Soc.* **132**, 8433–8439 (2010).
**This paper represents the first example of the imaging of enzyme catalysis involving the lipolysis of triglycerides within lipid droplets.**
39. Hellerer, T. *et al.* Monitoring of lipid storage in *Caenorhabditis elegans* using coherent anti-Stokes Raman scattering (CARS) microscopy. *Proc. Natl. Acad. Sci. USA* **104**, 14658–14663 (2007).
**This paper contains first examples of live whole organism imaging using CARS microscopy by examining processes involved in lipid storage in *Caenorhabditis elegans*.**
40. Kennedy, D.C., Lyn, R.K. & Pezacki, J.P. Cellular lipid metabolism is influenced by the coordination environment of copper. *J. Am. Chem. Soc.* **131**, 2444–2445 (2009).
41. Kim, S.H. *et al.* Multiplex coherent anti-Stokes Raman spectroscopy images intact atheromatous lesions and concomitantly identifies distinct chemical profiles of atherosclerotic lipids. *Circ. Res.* **106**, 1332–1341 (2010).
**This paper uses multiplex CARS microspectroscopy to identify and characterize the chemical profiles of four types of atherosclerotic lipids.**
42. Lee, B., Zhu, J.B., Wolins, N.E., Cheng, J.X. & Buhman, K.K. Differential association of adipophilin and TIP47 proteins with cytoplasmic lipid droplets in mouse enterocytes during dietary fat absorption. *Biochim. Biophys. Acta* **1791**, 1173–1180 (2009).
43. Lyn, R.K. *et al.* Direct imaging of the disruption of hepatitis C virus replication complexes by inhibitors of lipid metabolism. *Virology* **394**, 130–142 (2009).
**In this study, CARS microscopy is used to show drug-induced modulations of the host lipid environment and dispersal of HCV replication complexes.**
44. Pliss, A., Kuzmin, A.N., Kachynski, A.V., Prasad, P.N. Biophotonic probing of macromolecular transformations during apoptosis. *Proc. Natl. Acad. Sci. USA* **107**, 12771–12776 (2010).
45. Nan, X., Cheng, J.X. & Xie, X.S. Vibrational imaging of lipid droplets in live fibroblast cells with coherent anti-Stokes Raman scattering microscopy. *J. Lipid Res.* **44**, 2202–2208 (2003).
**This study demonstrated imaging of lipid droplets using CARS microscopy.**
46. Nan, X., Potma, E.O. & Xie, X.S. Nonperturbative chemical imaging of organelle transport in living cells with coherent anti-stokes Raman scattering microscopy. *Biophys. J.* **91**, 728–735 (2006).
47. Rinia, H.A., Burger, K.N.J., Bonn, M. & Muller, M. Quantitative label-free imaging of lipid composition and packing of individual cellular lipid droplets using multiplex CARS microscopy. *Biophys. J.* **95**, 4908–4914 (2008).
48. Robinson, I. *et al.* Intracellular imaging of host-pathogen interactions using combined CARS and two-photon fluorescence microscopies. *J. Biophotonics* **3**, 138–146 (2010).
49. Slipchenko, M.N., Le, T.T., Chen, H.T. & Cheng, J.X. High-speed vibrational imaging and spectral analysis of lipid bodies by compound Raman microscopy. *J. Phys. Chem. B* **113**, 7681–7686 (2009).
50. Zhu, J., Lee, B.G., Buhman, K.K. & Cheng, J.X. A dynamic, cytoplasmic triacylglycerol pool in enterocytes revealed by ex vivo and in vivo coherent anti-Stokes Raman scattering imaging. *J. Lipid Res.* **50**, 1080–1089 (2009).
51. Le, T.T., Huff, T.B. & Cheng, J.X. Coherent anti-Stokes Raman scattering imaging of lipids in cancer metastasis. *BMC Cancer* **9**, 42 (2009).
52. Bégin, S., Belanger, E., Laffray, S., Vallee, R. & Cote, D. *In vivo* optical monitoring of tissue pathologies and diseases with vibrational contrast. *J. Biophotonics* **2**, 632–642 (2009).
53. Chen, H. *et al.* Polyethylene glycol protects injured neuronal mitochondria. *Pathobiology* **76**, 117–128 (2009).
54. Evans, C.L. *et al.* Chemically-selective imaging of brain structures with CARS microscopy. *Opt. Express* **15**, 12076–12087 (2007).
55. Fu, Y., Wang, H.F., Huff, T.B., Shi, R. & Cheng, J.X. Coherent anti-stokes Raman scattering imaging of myelin degradation reveals a calcium-dependent pathway in lyso-PtdCho-induced demyelination. *J. Neurosci. Res.* **85**, 2870–2881 (2007).
**This study showed that demyelination of neurons can be detected using CARS microscopy.**
56. Huff, T.B. & Cheng, J.X. *In vivo* coherent anti-Stokes Raman scattering imaging of sciatic nerve tissue. *J. Microsc.* **225**, 175–182 (2007).

57. Wang, H., Fu, Y., Zickmund, P., Shi, R.Y. & Cheng, J.X. Coherent anti-stokes Raman scattering imaging of axonal myelin in live spinal tissues. *Biophys. J.* **89**, 581–591 (2005).
**This study demonstrated imaging of myelin using CARS microscopy.**
58. Kennedy, A.P., Sutcliffe, J. & Cheng, J.X. Molecular composition and orientation in myelin figures characterized by coherent anti-stokes Raman scattering microscopy. *Langmuir* **21**, 6478–6486 (2005).
59. Konorov, S.O. *et al.* *In situ* analysis of living embryonic stem cells by coherent anti-stokes Raman Microscopy. *Anal. Chem.* **79**, 7221–7225 (2007).
60. Noestheden, M. *et al.* Synthesis and characterization of CN-modified protein analogues as potential vibrational contrast agents. *Bioorg. Chem.* **35**, 284–293 (2007).
61. Pezacki, J.P., Singaravelu, R. & Lyn, R.K. Host-virus interactions during hepatitis C virus infection: a complex and dynamic molecular biosystem. *Mol. Biosyst.* **6**, 1131–1142 (2010).
62. Nan, X., Tonary, A.M., Stolow, A., Xie, X.S. & Pezacki, J.P. Intracellular imaging of HCV RNA and cellular lipids by using simultaneous two-photon fluorescence and coherent anti-Stokes Raman scattering microscopies. *ChemBioChem* **7**, 1895–1897 (2006).
**This paper describes the use of multimodal imaging to show how the hepatitis C virus perturbs the lipid metabolism of the host cell.**
63. Noestheden, M., Hu, Q.Y., Tonary, A.M., Tay, L.L. & Pezacki, J.P. Evaluation of chemical labeling strategies for monitoring HCV RNA using vibrational microscopy. *Org. Biomol. Chem.* **5**, 2380–2389 (2007).
64. Rakic, B. *et al.* Peroxisome proliferator-activated receptor alpha antagonism inhibits hepatitis C virus replication. *Chem. Biol.* **13**, 23–30 (2006).
65. Le, T.T., Duren, H.M., Slipchenko, M.N., Hu, C.D. & Cheng, J.X. Label-free quantitative analysis of lipid metabolism in living *Caenorhabditis elegans*. *J. Lipid Res.* **51**, 672–677 (2010).
66. Kang, E. *et al.* In situ visualization of paclitaxel distribution and release by coherent anti-stokes Raman scattering microscopy. *Anal. Chem.* **78**, 8036–8043 (2006).
**This report describes how the rate of drug release from a delivery polymer for paclitaxel can be monitored using CARS microscopy.**
67. Meyer, T. *et al.* Three-dimensional molecular mapping of a multiple emulsion by means of CARS microscopy. *J. Phys. Chem. B* **112**, 1420–1426 (2008).
68. Tong, L., Lu, Y., Lee, R.J. & Cheng, J.X. Imaging receptor-mediated endocytosis with a polymeric nanoparticle-based coherent anti-stokes raman scattering probe. *J. Phys. Chem. B* **111**, 9980–9985 (2007).
69. Windbergs, M. *et al.* Chemical imaging of oral solid dosage forms and changes upon dissolution using coherent anti-Stokes Raman scattering microscopy. *Anal. Chem.* **81**, 2085–2091 (2009).
70. Le, T.T., Yue, S.H. & Cheng, J.X. Shedding new light on lipid biology with coherent anti-Stokes Raman scattering microscopy. *J. Lipid Res.* **51**, 3091–3102 (2010).
71. Bonn, M., Muller, M., Rinia, H.A. & Burger, K.N.J. Imaging of chemical and physical state of individual cellular lipid droplets using multiplex CARS microscopy. *J. Raman Spectrosc.* **40**, 763–769 (2009).
72. Lyn, R.K., Kennedy, D.C., Stolow, A., Ridsdale, A. & Pezacki, J.P. Dynamics of lipid droplets induced by the hepatitis C virus core protein. *Biochem. Biophys. Res. Commun.* **399**, 518–524 (2010).
73. Freudiger, C.W. *et al.* Label-free biomedical imaging with high sensitivity by stimulated Raman scattering microscopy. *Science* **322**, 1857–1861 (2008).
**This paper demonstrates the principles of SRS microscopy.**
74. Saar, B.G. *et al.* Video-rate molecular imaging in vivo with stimulated Raman scattering. *Science* **330**, 1368–1370 (2010).
75. Pegoraro, A.F. *et al.* Optimally chirped multimodal CARS microscopy based on a single Ti:sapphire oscillator. *Opt. Express* **17**, 2984–2996 (2009).
**This study is the first demonstration of CARS microscopy with a single femtosecond laser light source, a photonic crystal fiber for generating the Stokes light and optical chirping to improve spectral resolution, the design that has led to the first commercially available CARS microscope.**
76. Wu, Y.M. *et al.* Quantitative assessment of hepatic fat of intact liver tissues with coherent anti-Stokes Raman scattering microscopy. *Anal. Chem.* **81**, 1496–1504 (2009).
77. Sowa, M.G. *et al.* Nonlinear optical measurements of the artery wall: parameters related to the progression of atherosclerosis. *Meas. Sci. Rev.* **9**, 93–94 (2009).
78. Evans, C.L. *et al.* Chemical imaging of tissue *in vivo* with video-rate coherent anti-Stokes Raman scattering microscopy. *Proc. Natl. Acad. Sci. USA* **102**, 16807–16812 (2005).
**In this report, live tissue is imaged at video rate to visualize rapid processes such as the penetration of oils into skin.**
79. Fu, Y., Sun, W.J., Shi, Y.Z., Shi, R.Y. & Cheng, J.X. Glutamate excitotoxicity inflicts paranodal myelin splitting and retraction. *PLoS ONE* **4**, e6705 (2009).
80. Yamaguchi, T. *et al.* CGI-58 facilitates lipolysis on lipid droplets but is not involved in the vesiculation of lipid droplets caused by hormonal stimulation. *J. Lipid Res.* **48**, 1078–1089 (2007).
81. Le, T.T. & Cheng, J.X. Single-cell profiling reveals the origin of phenotypic variability in adipogenesis. *PLoS ONE* **4**, e5189 (2009).
82. Huster, D. *et al.* High copper selectively alters lipid metabolism and cell cycle machinery in the mouse model of Wilson disease. *J. Biol. Chem.* **282**, 8343–8355 (2007).
83. Kolb, H.C., Finn, M.G. & Sharpless, K.B. Click chemistry: diverse chemical function from a few good reactions. *Angew. Chem. Int. Ed. Engl.* **40**, 2004–2021 (2001).
84. Xie, X.S., Yu, J. & Yang, W.Y. Perspective—living cells as test tubes. *Science* **312**, 228–230 (2006).
85. Ganikhanov, F., Evans, C.L., Saar, B.G. & Xie, X.S. High-sensitivity vibrational imaging with frequency modulation coherent anti-Stokes Raman scattering (FM CARS) microscopy. *Opt. Lett.* **31**, 1872–1874 (2006).
86. Li, L., Wang, H.F. & Cheng, J.X. Quantitative coherent anti-Stokes Raman scattering imaging of lipid distribution in coexisting domains. *Biophys. J.* **89**, 3480–3490 (2005).
87. Potma, E., de Boeij, W.P., van Haastert, P.J.M. & Wiersma, D.A. Real-time visualization of intracellular hydrodynamics in single living cells. *Proc. Natl. Acad. Sci. USA* **98**, 1577–1582 (2001).
**This paper is one of the first to demonstrate imaging of water and the effects that aquaporins have on water movement into cells by CARS.**
88. Chan, R.B., Tanner, L. & Wenk, M.R. Implications for lipids during replication of enveloped viruses. *Chem. Phys. Lipids* **163**, 449–459 (2010).
89. Miller, S. & Krijnse-Locker, J. Modification of intracellular membrane structures for virus replication. *Nat. Rev. Microbiol.* **6**, 363–374 (2008).
90. McLauchlan, J. Lipid droplets and hepatitis C virus infection. *Biochim. Biophys. Acta* **1791**, 552–559 (2009).
91. Gastaminza, P. *et al.* Cellular determinants of hepatitis C virus assembly, maturation, degradation, and secretion. *J. Virol.* **82**, 2120–2129 (2008).
92. Blais, D.R. *et al.* Activity-based protein profiling identifies a host enzyme, carboxylesterase 1, which is differentially active during hepatitis C virus replication. *J. Biol. Chem.* **285**, 25602–25612 (2010).
93. Elmén, J. *et al.* LNA-mediated microRNA silencing in non-human primates. *Nature* **452**, 896–899 (2008).
94. Jopling, C.L., Yi, M.K., Lancaster, A.M., Lemon, S.M. & Sarnow, P. Modulation of hepatitis C virus RNA abundance by a liver-specific microRNA. *Science* **309**, 1577–1581 (2005).
95. Kojima, S., Gatfield, D., Esau, C.C. & Green, C.B. MicroRNA-122 modulates the rhythmic expression profile of the circadian deadenylase nocturnin in mouse liver. *PLoS ONE* **5**, e11264 (2010).
96. Krützfeldt, J. *et al.* Silencing of microRNAs *in vivo* with 'antagomirs'. *Nature* **438**, 685–689 (2005).
97. Sagan, S.M. *et al.* The influence of cholesterol and lipid metabolism on host cell structure and hepatitis C virus replication. *Biochem. Cell Biol.* **84**, 67–79 (2006).
98. Le, T.T. *et al.* Nonlinear optical imaging to evaluate the impact of obesity on mammary gland and tumor stroma. *Mol. Imaging* **6**, 205–211 (2007).
99. Lim, R.S. *et al.* Multimodal CARS microscopy determination of the impact of diet on macrophage infiltration and lipid accumulation on plaque formation in ApoE-deficient mice. *J. Lipid Res.* **51**, 1729–1737 (2010).
100. Balu, M., Liu, G.J., Chen, Z.P., Tromberg, B.J. & Potma, E.O. Fiber delivered probe for efficient CARS imaging of tissues. *Opt. Express* **18**, 2380–2388 (2010).


## Acknowledgments

This work was supported by a grant from the Canadian Institutes of Health Research (CIHR) and Natural Sciences and Engineering Research Council (NSERC) of Canada. We thank D. Côté (Laval), A. Enejder (Chalmers), D.W. Moon (Korea Research Institute of Standards and Science) and M. Bonn (FOM Institute for Atomic and Molecular Physics) for contributing images to this review. We thank Y. Jia (Olympus America Inc.), A.F. Pegoraro (Queens University and National Research Council of Canada (NRC)), D. Moffat (NRC), A. Ridsdale (NRC) and A.D. Slepkov (NRC) for advice and help with CARS microscopy. R.S. thanks NSERC for a Vanier Graduate Scholarship and the CIHR National Canadian Research Training Program in Hepatitis C for additional support and training. D.C.D. thanks NSERC for a Canadian Graduate Scholarship. R.K.L. thanks the NSERC Collaborative Research and Training Experience Program in Medicinal Chemistry and Biopharmaceutical Development for support and training. J.P.P. would like to thank X.S. Xie and A. Stolow for many fruitful discussions and collaborations in CARS microscopy.

## Competing financial interests

The authors declare no competing financial interests.

## Additional information

Reprints and permissions information is available online at http://npg.nature.com/reprintsandpermissions/. Correspondence should be addressed to J.P.P.